

# ONGOING GALACTIC ACCRETION: SIMULATIONS AND OBSERVATIONS OF CONDENSED GAS IN HOT HALOS

J. E. G. PEEK<sup>1</sup>, M. E. PUTMAN<sup>2</sup>, JESPER SOMMER-LARSEN<sup>3,4</sup>

*Submitted to the Astrophysical Journal*

## ABSTRACT

Ongoing accretion onto galactic disks has been recently theorized to progress via the unstable cooling of the baryonic halo into condensed clouds. These clouds have been identified as analogous to the High-Velocity Clouds (HVCs) observed in HI in our Galaxy. Here we compare the distribution of HVCs observed around our own Galaxy and around the Andromeda galaxy to HVCs in a simulation of galaxy formation that naturally generates these condensed clouds. We find a very good correspondence between these observations and the simulation. We show that HVC accretion only accounts for  $\sim 0.2M_{\odot}$  / year of the current overall Galactic accretion. We also find that the simulated HVCs accelerate and become more massive as they fall toward the disk. The parameter space of the simulated clouds is consistent with all of the observed HVC complexes that have distance constraints, except the Magellanic Stream which is known to have a different origin. We also find that half of these simulated HVCs would be indistinguishable from lower-velocity gas and that this effect is strongest further from the disk of the galaxy. These results indicate that the majority of HVCs are consistent with being infalling, condensed clouds that are a remnant of Galaxy formation.

*Subject headings:* ISM: kinematics and dynamics, ISM: clouds, Galaxy: halo, galaxies: formation

## 1. INTRODUCTION

Galaxies have long been thought to form from the cooling of shock-heated primordial material in galactic halos (e.g. White & Rees 1978, White & Frenk 1991). These galaxy formation models, wherein all of the gas inside some time-dependent “cooling radius” monolithically collapses, cannot generate the continuous accretion needed to reproduce the Galaxy’s star-formation history (e.g. Rocha-Pinto et al. 2000). Maller & Bullock (2004) (hereafter MB04) showed that the process of the formation of galaxies could be driven by a multi-phase cooling process, in which not all of the gas within the cooling radius simply collapses (see also Kaufmann et al. 2005 and Sommer-Larsen 2006), but instead the hot ( $\sim 10^6$  K) shock-heated gas condenses out into warm ( $\sim 10^4$  K) clouds which fall inwards and collide, contributing to the formation of the galaxy. As time goes on, clouds condense at lower densities, corresponding to greater distances from the galactic center, and ‘rain’ inwards towards the disk. This formulation, wherein accretion is more continuous, avoids the “overcooling problem” that plagued monolithic collapse models. MB04 identified these condensations as being observable as High-Velocity Clouds (HVCs). This raised the exciting possibility that observations of HVCs can be used as a direct measure of the state of our Galaxy’s growth. We now further consider that we may be able to study galaxy formation quantitatively by studying various HVC observables and mapping them to the various parameters of galaxy for-

mation simulations. Such a course of study might help disentangle the large scale processes (cooling, merging, outflows, etc.) that shape today’s galaxy population.

HVCs have been known for over 40 years (Muller et al. 1963), having been first observed in the 21-cm hyperfine transition of neutral hydrogen. They are observed to be moving at hundreds of  $\text{km s}^{-1}$ , beyond what would be expected on the basis of Galactic rotation, with an overall sense of infall. Large maps have been made of the Galactic sky in HI (e.g. Putman et al. 2002, Kalberla et al. 2005), providing a good understanding of the gross observational characteristics of the HI HVCs. HVCs have also been observed in other atomic transitions (e.g. Sembach et al. 2003, Tripp et al. 2003), ionized gas (e.g. Putman et al. 2003, Tuftte et al. 2002) and there are tentative detections of dust as well (Miville-Deschênes et al. 2005). These observations are much more sparse than the HI observations, and do not give us a sense of the distribution of the entire HVCs population, though they provide some useful fiducial characteristics, such as metallicity (van Woerden & Wakker 2004) and rough estimates of ionization fraction (Tuftte 2004).

The origin and physical character of HVCs is still not known. The Magellanic Stream, a group of HVCs trailing the Magellanic Clouds, is certainly due to the interaction of the Galaxy and the Magellanic Clouds and may have come from some combination of ram-pressure stripping by the gaseous halo and tidal effects (Putman et al. 2003). Some Intermediate-Velocity Clouds (IVCs) have been shown to be very nearby ( $\sim 1$  kpc from the Galactic disk) and have near-solar metallicities, and are therefore thought to be part of a Galactic fountain, a formation scenario in which gas is kicked out of the disk and rains back down. The rest of the population of HVCs are thought either to be satellite debris akin to the Magellanic Stream or part of the cooling formation process. In the past both Galactic fountain models (e.g.

<sup>1</sup> Department of Astronomy, University of California, Berkeley, CA 94720

<sup>2</sup> Department of Astronomy, University of Michigan, 500 Church Street, Ann Arbor, MI 48109

<sup>3</sup> Dark Cosmology Centre, Niels Bohr Institute, Juliane Maries Vej 30, DK-2100 Copenhagen, Denmark

<sup>4</sup> Institute of Astronomy, University of Tokyo, Osawa 2-21-1, Mitaka, Tokyo, 181-0015, Japan

de Avillez 2000) and Local Group models, wherein HVCs are dark-matter dominated clouds hundreds of kpc from the Galaxy (e.g. Blitz et al. 1999), have also been invoked to explain HVCs. Neither of these models, though, is currently thought to be a successful explanation of the bulk of HVCs. Many HVCs have been shown to have distances beyond a few kpc (e.g. Thom et al. 2006, Wakker 2001), and low metallicities (for a review, van Woerden & Wakker 2004), which conflicts with the fountain model predictions of nearby, disk-like gas. Observations of Andromeda (Thilker et al. 2004, Westmeier et al. 2005) have excluded massive HVCs at great distances from that galaxy, which are a key prediction of Local Group models.

In an effort to understand the significance and scope of a Galactic gaseous halo, Sommer-Larsen (2006) (hereafter S-L06) ran numerical simulations of galaxy formation in the  $\Lambda$ CDM cosmology. These simulations showed that in Milky-Way-sized galaxies, significant baryonic mass resides in the hot halo. S-L06 also showed that infalling condensations are a natural consequence of such halos, and that it is possible to identify these clouds as HVCs.

In this paper we study the condensations found in S-L06 as HVCs and compare them to the HI HVC population in our Galaxy in terms of their number, flux and velocity distribution. We will also compare them to the HVC analogs observed around the Andromeda galaxy, which provides the opportunity to study the projected distance of HVCs, albeit with much lower resolution and sensitivity. We show that these condensations are indeed consistent with the overall HVC population and examine the simulation population for physical characteristics that may inform our future study of HVCs and ongoing galaxy formation.

## 2. OBSERVATIONS

### 2.1. *Selecting HVCs from Galactic Observations*

HVCs can be quantitatively defined in a variety of ways that reproduce the qualitative group of clouds traveling hundreds of  $\text{km s}^{-1}$  relative to Galactic rotation. It is important to realize that as HVCs are defined by their radial velocities (redshifts), and that as such any scheme will undoubtedly misclassify some objects with high true velocity as slower moving gas. Local Standard of Rest (LSR) velocities (which is to say heliocentric radial velocities corrected for the Sun’s peculiar motion as compared to the mean motion of stars in the stellar vicinity) have been used historically to define the difference between HVCs and other Galactic clouds. Unfortunately, the rotation of the Galaxy will contaminate the sample of clouds, particularly towards ( $l = 90$ ) and away from ( $l = 270$ ) the direction of Galactic rotation. Classifying by Galactic Standard of Rest (GSR) velocities avoids some of these problems by moving into a frame at rest with respect to the Galaxy, but the disk gas contamination is still a strong function of angle on the sky, either requiring very harsh cuts ( $|v_{\text{GSR}}| > 220 \text{ km s}^{-1}$ ) or including a large amount of gas plainly part of the disk in the quadrants I and IV. A solution to this conundrum is the parameter  $v_{\text{dev}}$ , which is a measure of how the velocity of a cloud deviates from a relatively simple model of the Galactic disk. The model includes solid-body rotation

in the Galactic center, a flat rotation curve at larger  $R$  and a flared disk (see Wakker 2004 for details). We use the criteria  $|v_{\text{dev}}| > 60 \text{ km s}^{-1}$  and  $|v_{\text{LSR}}| > 90 \text{ km s}^{-1}$ , both to excerpt the disk and to fulfill the classical definition of HVCs. These criteria are applied to observed and simulated HVCs alike. The  $|v_{\text{LSR}}| > 90 \text{ km s}^{-1}$  has a very limited effect upon the selected complexes once the  $|v_{\text{dev}}| > 60 \text{ km s}^{-1}$  is applied (it removes only one complex) and our results do not significantly depend upon whether the  $|v_{\text{LSR}}| > 90 \text{ km s}^{-1}$  is applied.

As we are interested in the global properties of HVCs rather than their minutiae, which are beyond the resolution of the simulation, we wish to use a full sky survey with consistent resolution and nomenclature. For this reason we use the updated Wakker and Van Woerden catalog (Wakker & van Woerden 1991). This catalog has the velocities, fluxes and positions of more than 600 clouds; Wakker (2004) uses this same sample, and a more detailed description can be found therein. This catalog includes all clouds that have historically been catalogued as HVCs, and we exclude those clouds that do not fit our criteria for HVCs mentioned above. The 475 individual clouds that meet our criteria have an unweighed mean of  $-61 \text{ km s}^{-1}$  GSR and a standard deviation of  $101 \text{ km s}^{-1}$  GSR.

Most of the HI flux of HVCs comes from HVC “complexes”: individual clouds that are members of a larger group of clouds in the same region of the sky with similar velocities. Clouds in the updated Wakker & Van Woerden catalog are labeled by the complex to which they belong, if any. There are independent clouds as well, but they make up a small fraction of the overall observed distribution.

The complex is the largest cohesive HVC grouping; we will use it as our fundamental unit for comparison to the simulation. We do not address the possibility that small, isolated clouds may be their own complex analogs at great distance. Indeed, if all such small clouds were distant complex analogs they should be reproduced by the simulation, and a comparison of small, isolated clouds would be fruitful. Many such observed clouds, though, may simply be physically small, nearby clouds. These nearby clouds would not be reproduced by the simulation, being below the simulation resolution limit, and would thus contaminate any comparison. We ignore them here for this reason.

Beyond excluding all small, isolated clouds from the comparison we also exclude complexes which have known, inconsistent origins. These are the “Outer Arm” complex, thought to be part of the warp of the Galactic disk; the “Magellanic Stream” and “Leading Arm” complexes, known to have originated in the Magellanic clouds; and all “Intermediate Velocity” clouds, which are thought to have come as an ensemble from the Galactic disk, owing to their high metallicity and proximity. Once we have eliminated irrelevant complexes, we are left with 14 HVC complexes.

### 2.2. *HVCs around the Andromeda galaxy*

In addition to Galactic observations of HVCs, analogs to HVCs have been discovered in other galaxies and, in particular, recent observations of Andromeda (M31) have shown a large number of distinct complexes (Thilker

et al. 2004) (hereafter T04). The T04 observations are the most comprehensive study of extragalactic HVCs and have enough sensitivity to detect a large fraction of HVCs from the S-L06 simulations. These observations have an advantage over Galactic observations in that they have a projected galacto-centric radial distance for each cloud, as well as a relatively accurate distance and therefore HI mass for the clouds. At a distance of 775 kpc Andromeda is the nearest spiral galaxy to our own Milky Way. With a mass comparable to that of the Milky Way (Seigar et al. 2006), and without evidence of recent major mergers, we expect Andromeda to have a relatively similar recent formation history, and therefore a similar population of HVCs, to our own Galaxy. The T04 observations cover a 94 kpc  $\times$  94 kpc square at Andromeda which, though smaller than the simulation domain, overlaps with the bulk of the simulated clouds. The resolution is 2 kpc with capacity to detect clouds down to a few  $\times 10^5 M_\odot$  of HI, depending upon their size, which is comparable to the mass resolution of the simulation. These observations (along with Westmeier et al. 2005) show that there exists a significant population of HVCs within 50 kpc of Andromeda’s disk, with masses ranging from the sensitivity limit up to  $10^7 M_\odot$ , and that there are not HVCs with masses  $\geq 10^6 M_\odot$  outside  $R = 50$  kpc; these are significant constraints to which we can compare the simulations.

### 3. SIMULATIONS

The code used for the simulations is a significantly improved version of the TreeSPH code, which has been used previously for galaxy formation simulations (Sommer-Larsen et al. 2003). The main improvements over the previous version are: (1) The “conservative” entropy equation solving scheme suggested by Springel & Hernquist (2002) has been adopted. (2) Non-instantaneous gas recycling and chemical evolution, tracing 10 elements (H, He, C, N, O, Mg, Si, S, Ca and Fe), has been incorporated in the code following Lia et al. (2002b) and Lia et al. (2002a); the algorithm includes supernovae of type II and type Ia, and mass loss from stars of all masses. (3) Atomic radiative cooling depending both on the metal abundance of the gas and on the meta-galactic UV field, modeled after Haardt & Madau (1996) is invoked, as well as simplified treatment of radiative transfer, switching off the UV field where the gas becomes optically thick to Lyman limit photons on scales of  $\sim 1$  kpc.

Sommer-Larsen (2006) selected a Milky-Way-like galaxy from a cosmological simulation and simulated its gaseous halo at extremely high resolution. The purpose of the experiment was to establish how large a mass fraction of the hot gas halos, shown to contribute significantly to the baryonic mass budget of such galaxies, condense into “warm” ( $T \sim 10^4$  K) clouds by thermal instability. The result of the experiment was that only a few percent of the hot gas mass forms warm clouds; it was suggested that these clouds would be the equivalent of the HVCs. For the purpose of this paper, specifically addressing the properties of these warm clouds, an enlarged version of the above simulation was performed.

The base of the experiment was a  $3.2 \times 10^5$  particle, fully cosmological simulation of a disk galaxy, which at  $z=0$  has a characteristic circular velocity of  $V_c=224$  km/s, very similar to that of the Milky Way. At  $t=10.0$

Gyr ( $z \sim 0.3$ ), all gas particles within 250 kpc galacto-centric distance are split in eight particles of mass 1/8th the original value and gravity softening length (inverse gravity force resolution) 1/2 of the original value. The simulation is then continued for 200 Myr, and then all gas particles within 100 kpc galacto-centric distance are again split in eight particles of mass 1/8 and gravity softening length 1/2 of the previous values. At this point the simulation totals  $1.1 \times 10^6$  particles, of which  $8.6 \times 10^5$  are gas particles. The warm/hot gas in the inner 100 kpc of the galaxy halo is then resolved with particles of mass  $m_{\text{gas}}=11700 M_\odot$  and gravity softening length 128 pc. As discussed by Sommer-Larsen (2006) this enables the simulation to resolve HVCs down to masses of  $\sim 3 \times 10^5 M_\odot$  within 100 kpc galacto-centric distance. The (by now) very high resolution simulation is run for 500 Myr, until  $t=10.7$  Gyr, at which point it was terminated due to the heavy computational load. By  $t=10.3$  Gyr more than 100 potential HVCs have formed, with the number increasing slightly over the next 300 Myr. All HVCs are found at galacto-centric distances less than 100 kpc, no HVCs were found in the region  $100 < r \lesssim 250$  kpc down to the mass resolution of  $\sim 3 \times 10^6 M_\odot$  in this region of the halo (Sommer-Larsen 2006). We note that the necessary condition for onset of thermal instability, viz.  $\tau_\lambda < \tau_{\text{cool}}$ , is satisfied everywhere in the hot halo gas ( $\tau_\lambda$  is the sound crossing time, which is taken to be  $\sim 2h_{\text{SPH}}/c_s$ , where  $h_{\text{SPH}}$  is the local SPH smoothing length and  $c_s$  is the sound speed;  $\tau_{\text{cool}} = \frac{E}{\dot{E}}$  is the timescale for radiative cooling).

The bulk of the HVCs appear to have been seeded by remains from “cold accretion” events taking place much earlier in the history of the galaxy, as discussed by Sommer-Larsen (2006). However, given the much lower resolution of the main underlying galaxy simulation, starting at  $z_i=39$  and running to  $t=10.0$  Gyr, it is not possible to give a detailed discussion of the origin of the HVCs on the basis of the present simulations. These constraints also imply that the results obtained in this paper should, in general, be regarded as preliminary. Eventually, simulations starting at early times and of yet higher resolution should be undertaken, although such simulations are unfortunately computationally prohibitive at present.

#### 3.1. Selecting individual HVCs from the simulation

We identified potential halo HVCs in three snapshots at 300, 400 and 600 Myr ( $t=10.3$ , 10.4 and 10.6 Gyr). First, all “seed” SPH particles in the halo, satisfying  $n_H > n_{H,\text{trig}}$  and  $T < 3 \times 10^4$  K, were identified. Second, a gas particle group finder was used to identify all SPH particles in coherent regions in the halo, surrounding these “seed” particles, and satisfying  $n_H > n_{H,\text{min}}$ . Third, only SPH particles in these regions satisfying  $T < 3 \times 10^4$  K were retained. It is found that with  $n_{H,\text{trig}} \sim 10^{-2} \text{cm}^{-3}$  and  $n_{H,\text{min}} \sim 10^{-3.5} \text{cm}^{-3}$  one identifies neutral or partly photo-ionized  $T \sim 1\text{--}3 \times 10^4$  K gas in HVCs and satellite galaxies (SPH particles in the coherent regions of  $T \geq 3 \times 10^4$  K typically have  $T \sim 10^6$  K and are almost fully collisionally ionized), hence these density thresholds were adopted. Subsequently, the 7 satellite galaxies identified around this galaxy are removed on the basis of these systems containing (1) gas of high central density ( $n_H \gtrsim 1\text{--}10$

$\text{cm}^{-3}$ ), (2) stars and (3) dark matter.

### 3.2. Physical characteristics of simulated HVCs

The three snapshots in the simulation (300, 400 and 600 Myrs) have 113, 128 and 130 identified HVCs, respectively. Sommer-Larsen (2006) describes the mass distribution of the clouds in the simulation, which is consistent from snapshot to snapshot. HVC masses range from  $10^5 M_\odot$  to  $5 \times 10^6 M_\odot$ , with total masses ranging from  $8.8 \times 10^7 M_\odot$  to  $10.7 \times 10^7 M_\odot$ . Note that this total mass is much lower than the  $\sim 2 \times 10^{10} M_\odot$  proposed in MB04. Figure 1 shows the distribution of HVCs in the three snapshots, indicating both masses and velocity vectors. Note that the HVCs in each snapshot are not independent; a typical cloud moving at  $100 \text{ km s}^{-1}$  will only traverse 30 kpc from the first to last snapshot, so large structures that are consistent from snapshot to snapshot may indeed be related. The cloud distributions are roughly spherically symmetric and have an overall sense of infall. Clouds tend to have velocity vectors similar to their neighbors and show large-scale ( $\sim 30 \text{ kpc}$ ) inflow structures. This is worthy of note as large, coherent structures in HVCs are sometimes cited as qualitative evidence of a satellite-accretion origin. Figure 2 shows the number density and mass density profiles of each of the snapshots. We note that the 300 Myr snapshot has a noticeably lower number and mass density of clouds near the disk. This effect is consistent with not enough time having elapsed since the beginning of the highest resolution simulation for the most massive clouds to have formed and fallen into the center of the potential. The 400 Myr and 600 Myr snapshots have very similar density structures, indicating a converged and continuous HVC lifecycle.

In Figure 3 we plot the distribution of true-space velocity with respect to galactocentric radius of the HVCs for each of the three snapshots. The most striking feature of this plot is the increasing velocity of clouds with decreasing radius, consistent over time, which is also visible in Figure 1. This should not be a terribly surprising result, as clouds deeper in a galactic potential will typically have more kinetic energy, but the simple idea that more distant clouds may have velocities that are less extreme than other HVCs has not been much addressed in the study of HVCs to date. Also evident in Figure 3 is that at a given distance, more massive clouds typically move faster. This effect consistent with the supposition that drag from the gaseous halo on HVCs has a significant kinematic effect, and that more massive clouds typically have higher column densities.

### 3.3. Creating complexes from simulated HVCs

The contrast between the 14 observed complexes and the 113, 128 and 130 simulated HVCs is not quite as great as it seems because a large fraction of those simulated HVCs would actually not be observably distinguishable from disk gas, Low-Velocity Clouds (LVCs) or IVCs. If we position a theoretical earth at  $R=8.5 \text{ kpc}$  within the simulated disk and “observe” the radial velocities of these clouds we can apply radial velocity cuts consistent with HVC surveys. With these cuts, the number of clouds that would be seen as HVCs are  $54 \pm 6$ ,  $63 \pm 11$  and  $71 \pm 8$ , respectively. The variability in this quantity, and

other “observed” quantities we investigate, comes from the angle,  $\phi$ , around the galaxy center at which the Sun is positioned.

If in the simulation there were no clustering on the sky of HVCs in angle-velocity space, then the strong contrast between many dozens of simulated and observable HVCs and 14 observed complexes would convince us that the simulation was not capturing the physical picture correctly. In fact, it is visually evident that there is significant clustering of HVCs in the simulation that either were born as a single cloud and shattered or were created in some coherent ‘cooling flow’. These clouds should be treated as single entities, comparable to observed complexes. To decide which simulated clouds should be associated in this way we define a ‘distance measure’ in position-velocity space between clouds:

$$D = \sqrt{\Theta^2 + f^2 (\delta v)^2}. \quad (1)$$

Here,  $\Theta$  is the angular distance between two clouds,  $\delta v$  is the difference in velocity between two clouds and  $f$  is a conversion factor;  $f$  parameterizes the significance we ascribe to the angle subtended by two clouds versus their difference in velocity in determining whether they are members of the same complex. We choose  $f = 0.5^\circ / \text{km s}^{-1}$ , broadly consistent with the clustering in observed HVC complexes. We place two clouds in the same complex if their  $D$  is less than some number,  $D_0$ . A cloud with no neighbors is considered a complex of its own. The overall complex position and velocity are determined by a flux-weighted average of the constituent clouds, consistent with the method applied to the observed population.

This formulation leaves us with a free parameter,  $D_0$ . As  $D_0$  is increased the number of complexes decreases roughly linearly for reasonable values of  $D_0$ , thus the data do not offer a specific scale at which cloud clustering takes place. We wish to choose  $D_0$  such that we maximize the identification of true complexes and minimize the identification of complexes that are the result of coincidental cloud superposition. To that end we scramble all of the positions (l and b) and velocities ( $v_{\text{obs}}$ ) of the simulated clouds in each snapshot, such that all of the coherent angular and velocity structures are lost, while maintaining the distribution of each of these parameters individually. We then run the clustering algorithm on both the scrambled and unscrambled data sets for all values of  $D_0$ . We assume that any complexes generated in the scrambled data sets are spurious and we find the average  $D_0$  at which the difference in clustering, as parameterized by the number of complexes, is greatest between the true and scrambled data sets. This maximum occurs at  $D_0 \simeq 25^\circ$ , with little variation across the three snapshots. We adopt this value for generating simulated cloud complexes hereafter.

## 4. ANALYSIS

### 4.1. Comparing Observed Milky Way and Simulated HVCs

First we wish to compare the number and angular size of observed HVC complexes to the simulated complexes. Figure 4 shows each of the snapshots as observed from the Sun along with the observed HVC data. The number of complexes is similar,  $18.7 \pm 1.4$ ,  $22.6 \pm 2.6$  and

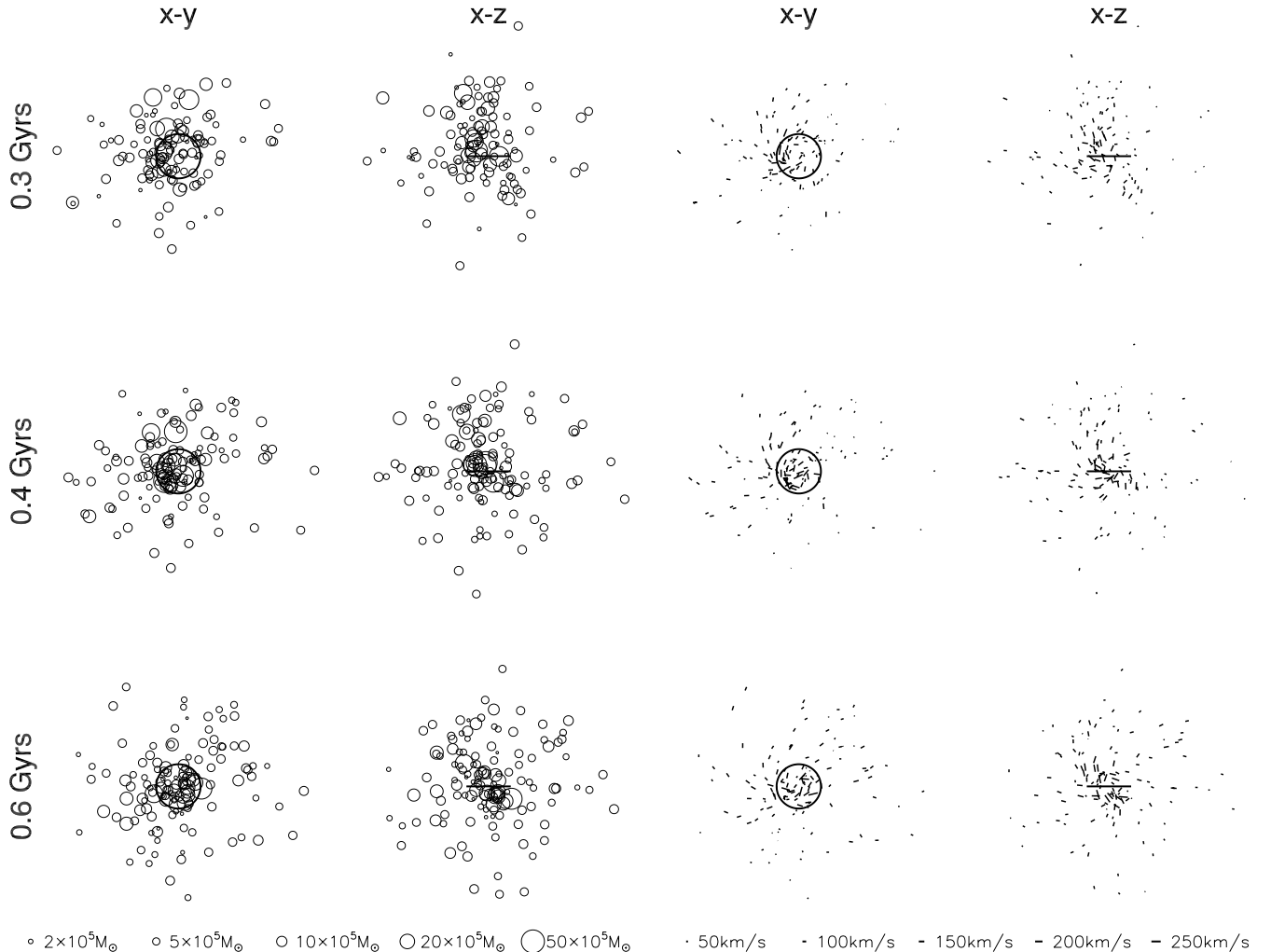


FIG. 1.— The distribution of simulated HVCs in the three snapshots, showing HVC mass (left) and velocity (right). Each snapshot is projected onto the x-y and y-z planes, and shows a ring of radius 15 kpc centered in the galactic plane for scale and orientation. Symbol area scales with the mass of the clouds at left, and symbol length scales with the velocity at right.

$25 \pm 1.7$  for the 300, 400 and 600 Myr snapshots respectively, as compared to 14 in the updated Wakker and Van Woerden catalog. While the numbers of simulated complexes observed are very similar to observations, we do see consistently more simulated complexes than observed complexes, by 25% to 80%. This may be a preliminary indication that there exists variation in ionization fraction across complexes; if some complexes are completely ionized and some dominantly neutral, the number of HI-observable complexes would go down as compared with a consistent ionization fraction across clouds. The effect may also stem from the difficulty in discerning the difference between small complexes and isolated clouds: we discard isolated clouds from the observed data set, but include small complexes. It may be that it is difficult to draw that distinction in the updated Wakker & van Woerden (1991) data set. Some subtle evolution exists in the number of clouds and complexes in the simulation data, consistent with the halo requiring more than 300 Myrs to reach an equilibrium in the condensation of HVCs after

the simulation has been run at high-resolution. Note that there are far more small clouds associated with a given complex in the real data, consistent with the limited resolution of the simulation. Also note that the simulated complexes have roughly similar angular distribution and size on the sky to those that are observed. In Figure 5 we show simulated complexes from four vantage points at the solar circle for each snapshot, demonstrating the variation in the distribution of complexes as a function of solar position.

We also wish to compare the velocities and fluxes of the simulated and observed HVCs. Fluxes are determined by assuming the gas in HVCs is 70% hydrogen by mass (consistent with Big Bang nucleosynthesis), and that the clouds are optically transparent to 21-cm radiation. This transparency assumption is reasonable as HVCs have a peak brightness temperature of a few K and a spin temperature upwards of 1000 K (see Kulkarni & Heiles (1988) for a discussion of the details of HI radiative transfer). Figure 6 shows the fluxes and veloc-

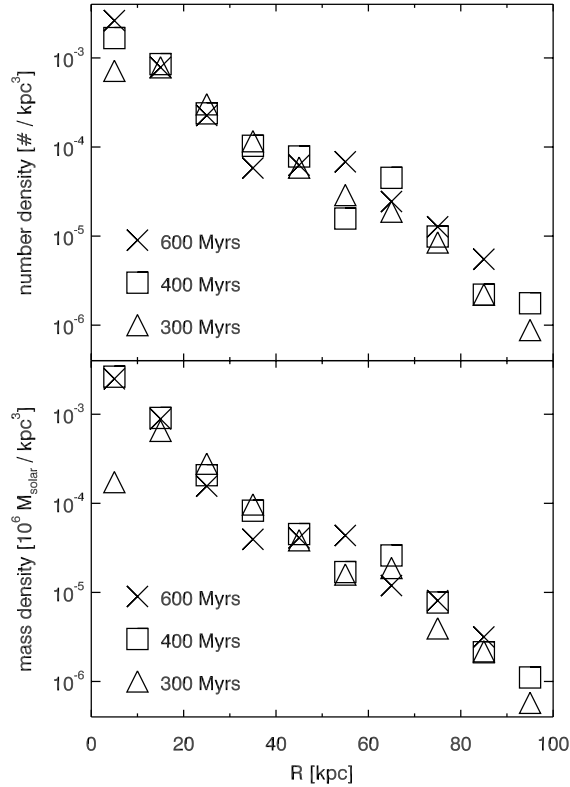


FIG. 2.— The number density (top) and mass density (bottom) profiles for the simulated HVCs with galactocentric radius, in 10 kpc bins. Each of the snapshots is plotted. There are no clouds between 90 and 100 kpc in the 600 Myr snapshot, as compared to 1 and 3 clouds in the 300 and 400 Myr snapshots respectively.

ities of each of the snapshots from four vantage points around the solar circle, along with the real HVC data. The total maximum HI flux in the simulated complexes are  $3.2 \pm 1.3$ ,  $7.8 \pm 3.6$  and  $6.3 \pm 2.2 \times 10^5$  Jy km/s, as compared to  $5.0 \times 10^5$  Jy km/s in the compared sample of real HVC complexes. Note that the maximum flux comes from the assumption that none of the cloud is ionized, therefore if a large fraction ( $\sim 70\%$ ) of the simulated HVCs were indeed ionized, simulation and observation would have significant discrepancy in HI flux. The range in total flux within a single snapshot is due to the fact that  $\sim 50\%$  of the overall flux comes from just a few complexes closer than 10 kpc; as the observation point is rotated around the Galaxy, the distance to these complexes changes, changing the overall flux. This dependence upon only a few large, local clouds diminishes the usefulness of flux as a measure of the accuracy of the simulations. The average velocities (GSR) are also similar:  $-71 \pm 11$ ,  $-82 \pm 16$  and  $-71 \pm 21$  km s $^{-1}$ , as compared to  $-68$  km/s in the observed complex dataset. The standard deviation of the distribution of cloud velocities is  $63 \pm 9$ ,  $81 \pm 12$  and  $81 \pm 8$  km s $^{-1}$ , as compared to 86 km/s in the observed complex data set. None of these distributions of observables contradict the hypothesis that the HVCs in the S-L06 simulations are analogous to the Milky Way’s population of HVCs.

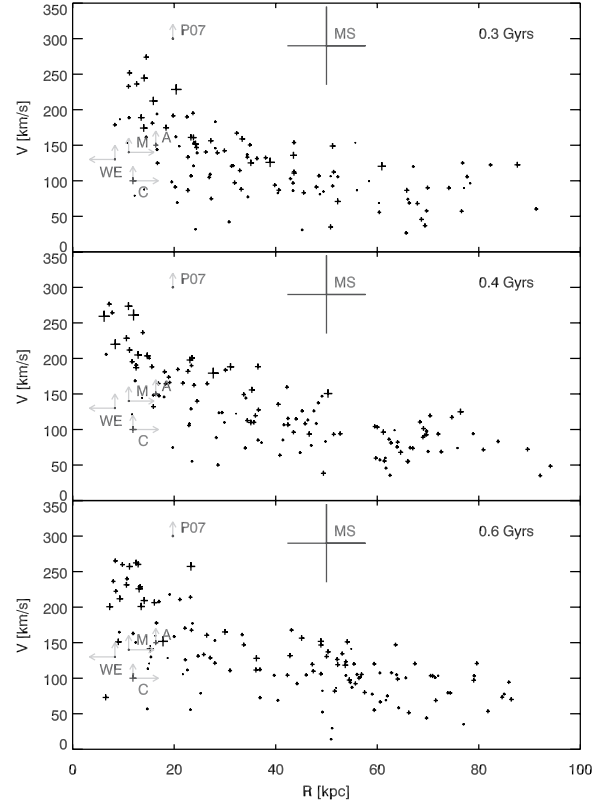


FIG. 3.— Three plots of HVC galactocentric radius versus true velocity (with respect to the center of mass of the Galaxy) of the three snapshots in the S-L06 simulation. The linear size of the symbol scales as the square-root of the mass of the cloud. Six observed clouds and complexes that have distance constraints are over-plotted (data from van Woerden & Wakker (2004) and Weiner et al. (2001)), with arrows indicating where values are only upper or lower limits in distance or lower limits in velocity. Clear trends of velocity with radius, mass with radius and velocity with mass at a fixed radius are evident.

#### 4.2. Comparing Andromeda’s HVCs with simulated HVCs

We compare observed quantities in the T04 Andromeda dataset to our simulated data set. T04 find that there is  $\sim (3 - 4) \times 10^7 M_\odot$  in HI mass around Andromeda; we find  $6.1$ ,  $7.5$  and  $6.8 \times 10^7 M_\odot$  in our 3 simulation snapshots of 300, 400 and 600 Myrs. This implies an ionization fraction ranging from 35% to 60% for the simulations to be consistent with the observations. The standard deviation of the projected velocities in the T04 Andromeda dataset is 126 km/s, although limiting the sample to objects with masses greater than  $5 \times 10^5 M_\odot$ , where we expect the sample to be complete, reduces this to 96 km/s. Also note that this velocity dispersion only pertains to the qualitatively-defined “objects” in the dataset, which excludes diffuse gas closer to the Andromeda disk. The simulation snapshots, once projected to mimic the Andromeda viewing angle, have velocity standard deviations of 63, 71 and 89 km s $^{-1}$ .

The spatial distribution of the HVCs is one of the most interesting quantities to pursue in this comparison, as the Andromeda data set yields a minimum galactocentric distance for all observed clouds, a quantity not afforded by the Galactic data set. It is, unfortunately, a rather

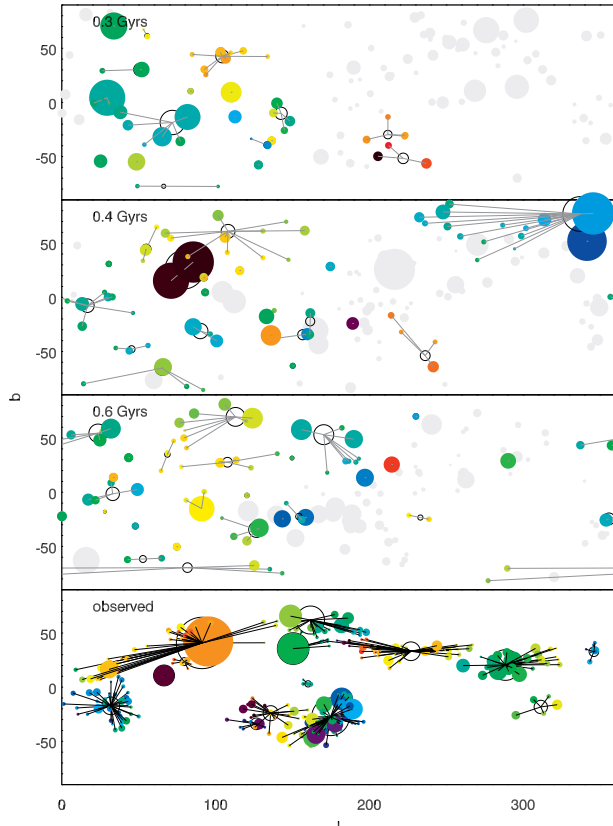


FIG. 4.— Four plots of HVC complex distribution on the Galactic sky. The first three are from the S-L06 simulations and the final plot is of the observed HVC complexes. Filled circles represent HVCs, with gray representing clouds not included in our sample and the linear size of the circle scaling with the cube-root of the HI flux, as HI flux covers more than 3 orders of magnitude. In the simulation plots, clouds are gray if they do not fulfill the velocity selection criteria:  $|v_{\text{dev}}| > 60 \text{ km s}^{-1}$  and  $|v_{\text{LSR}}| > 90 \text{ km s}^{-1}$ . Clouds are colored by their velocities, and we assume a neutral fraction of 50% in the simulation plots. Lines connect clouds to the flux-weighted centers of the complexes to which they belong. Complexes are indicated by an empty circle, with fluxes scaling the same way with circle size. Note that the lack of tiny clouds in simulated data is an expected consequence of the resolution limitations of the simulation.

difficult quantity to extract, as the scale of distribution of the halo is very sensitive to the sensitivity of the observations to small clouds, which is difficult to accurately characterize in these observations. We can conclude that both the Andromeda data set and the simulation snapshots have detectable HVCs out to projected galactocentric radii of 50 kpc, and lack clouds with  $M > 10^6 M_{\odot}$  outside 50 kpc. A more detailed analysis of the scale-length and HVC density profile, including lower mass clouds, will have to wait for deeper, higher resolution observations.

#### 4.3. The HVC Accretion Rate

Material cools out of the halo at different radii, allowing us to parameterize the HVC accretion rate onto the Galaxy as a function of radius in the simulations. At  $R=100$  kpc the accretion rate is zero, and at  $R=0$  kpc it is maximal. We define the HVC accretion rate at a given

galacto-centric radius by

$$\dot{M}(R) = \sum_{i=1}^{i=n(R)} \frac{M_i \vec{V}_i \cdot (-\hat{r}_i)}{dR}, \quad (2)$$

where  $M_i$  is the mass of a cloud,  $\vec{V}_i$  is a cloud velocity and  $\hat{r}_i$  is the radial unit vector at the cloud.  $n(R)$  is the number of clouds that exist in a spherical shell from  $R - dR/2$  to  $R + dR/2$ .  $\dot{M}(R)$  is not a well-defined metric within 10 kpc of the Galactic Center, as some of the HVCs will be removed from the system when they collide with the disk, so we exclude HVCs within 10 kpc from this analysis. We find that this HVC accretion rate, averaged over all three snapshots, can be easily fit by a line with  $\dot{M}(0) = 0.22 \pm 0.014 M_{\odot}/\text{year}$  and  $d\dot{M}(R)/dR = -2.5 \times 10^{-3} \pm 2 \times 10^{-4} M_{\odot}/\text{year/kpc}$ . This disk accretion rate of  $0.22 M_{\odot}/\text{year}$  is consistent with the assertion that HVC accretion is not the sole source of fuel for Galactic star formation (see Putman 2006 and Sommer-Larsen 2006). The monotonic increase in accretion rate with decreasing radius demonstrates that the cooling process that fuels HVC formation and growth operates at all radii within the halo.

## 5. DISCUSSION

### 5.1. The True Velocity Domain

The distribution that the simulated clouds present (see Figure 3) has a very clear variation of true velocity with galactocentric radius. Only one observed complex in the Galactic sky significantly strays from this region: the Magellanic Stream. This discrepancy, of course, does not contradict the hypothesis that the rest of the HVCs are generated by a mechanism similar to the one that generated the S-L06 HVCs; the Magellanic Stream was excluded from the analysis for the specific reason that it does have a well-known, non-cooling origin. The deviation of the Magellanic Stream from this area does indicate, however, that HVCs that are generated from satellite accretion may occupy a different part of the radius-velocity parameter space and that it therefore may be possible to distinguish the origin of an individual cloud if these values can be measured. Unfortunately, it is typically very difficult to measure cloud true velocity, or, equivalently, the angle that a cloud velocity vector makes with an observer-cloud vector, without strong model assumptions.

It is worth noting that the Very High-Velocity Cloud (VHVC) sub-complex that includes HVC 160.7-44.8-333 (annotated P07 in Figure 3) has been shown to have a galactocentric distance of  $\sim 20$  kpc (Weiner et al. 2001; Peek et al. 2007). At a minimum velocity of  $300 \text{ km s}^{-1}$  GSR, it is also marginally outside of the domain of clouds that are generated in the S-L06 simulations. Further distance limits on VHVCs may help to show whether these clouds are broadly inconsistent with cooling formation scenarios. Observations of VHVCs are particularly important as they have very large minimum true velocities, and are therefore plausibly excludable from the cooling-formation-origin domain. The vast majority, though, of the observed HVCs with distance constraints are consistent with the simulated HVCs.



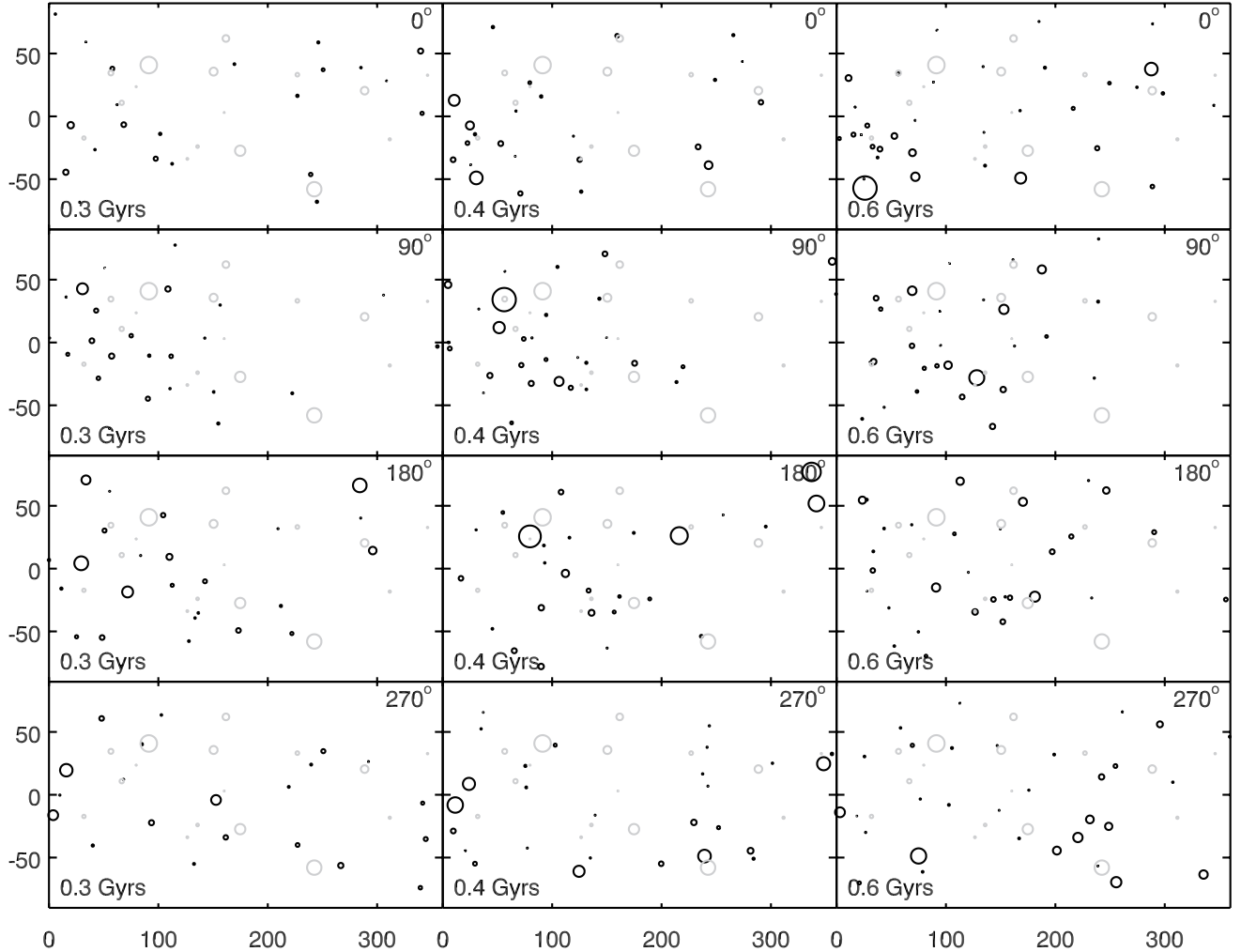


FIG. 5.— Twelve plots of Galactic  $l$  versus Galactic  $b$  for simulated HVC complexes. Columns from left to right are from each sequential snapshot (0.3, 0.4 and 0.6 Gyrs into the high-resolution simulation), and rows are from positions rotated by  $90^\circ$  around the solar circle. The symbol area scales with flux. Dark symbols represent simulated complexes and light symbols represent observed Galactic complexes, for comparison. Symbols are scaled using 50% neutral fraction. Note that the distribution of simulated complexes varies significantly with position of the Sun within the solar circle, but that the simulated complex distributions are all qualitatively similar to the observed complex distribution.

### 5.2. HVCs at Low Velocity

A crucial byproduct of the analysis of simulated condensed clouds as observable HVCs is that *fully half* of all simulated clouds that have HVC physical characteristics would not satisfy the observational criteria for HVCs. Instead, these clouds would be construed as lower-velocity (and therefore nearby) gas. This is to say that if all HVCs are generated by processes similar to those in the S-L06 simulations we are ‘missing’ as many HVCs as we observe and thus underestimate the total scale of HVCs by a factor of two. This effect increases with greater radius - the average velocity of clouds decreases with radius (see Figure 3), such that more distant clouds will be more often confused with local gas. The low apparent velocity clouds are startlingly asymmetrical. The ratio of the number of condensed clouds above  $|b|$  of  $50^\circ$  with  $-50 \text{ km s}^{-1} < V_{GSR} < 0 \text{ km s}^{-1}$  to clouds with  $0 \text{ km s}^{-1} < V_{GSR} < 50 \text{ km s}^{-1}$  is  $7 \pm 4$ ,  $9 \pm 3$  and  $11 \pm 3$  for each

of the snapshots. If these clouds could be observationally deciphered from nearby LVCs, this asymmetry could be a powerful test of this model for HVC formation. It may be possible in the future to disentangle such clouds from local gas via their morphological characteristics, absorption to stars, low metallicity and very low dust-to-gas ratio.

### 5.3. CHVC hypotheses

Compact high-velocity clouds (CHVCs), are HVCs that are smaller than about  $2^\circ$  in projected size and are not associated with other HVCs in the sky. CHVCs have received significant attention in recent years (e.g. Braun & Burton 1999) under the assumption that some or all of them are analogous to the observed large complexes of HVCs but at much greater distances. Were this true, CHVCs could dominate the mass of Galactic HVCs, and would be very important to understanding



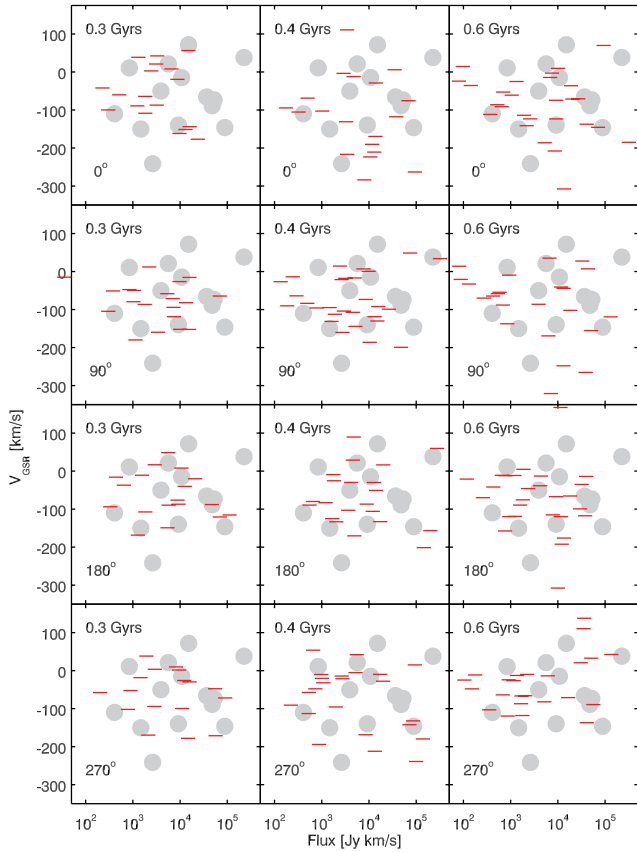


FIG. 6.— Twelve plots of GSR velocity versus HI flux for simulated HVC complexes and observed HVC complexes. In each plot the observed HVC complexes are depicted by gray filled circles for comparison. The dashes represent simulated complexes, with the right side of the dash representing 0% ionization and the left side of the dash representing 50% ionization. From left to right the plots are of 300, 400 and 600 Myrs into the simulation. From top to bottom the plots represent viewpoints of  $0^\circ$ ,  $90^\circ$ ,  $180^\circ$  and  $270^\circ$  around the solar circle.

the structure of the HVCs and the Galactic halo. This assumption hinges on the relative homogeneity of HVCs across distance. If HVCs have a distribution similar to the simulated distribution, this assumption would prove false. The most massive HVCs in the S-L06 simulations are typically closest to the disk, and they do not have analogs 50 to 100 kpc from the galaxy. In addition to this, the simulated velocity distribution of local HVCs is not analogous to that of distant HVCs; distant HVCs move slower, thus if some CHVCs are indeed distant objects (and the cooling-formation predictions are correct) there will exist a trend toward lower velocities in CHVCs. CHVC catalogs do not show a lower velocity dispersion than catalogs of HVCs (Putman et al. 2002), but such a discrepancy may be hard to detect as small, local clouds may masquerade as distant CHVCs (thus polluting the sample; see discussion in Section 2.1) and disk gas may obscure a large fraction of the population of slow-moving, distant CHVCs. Conversely, it is possible to limit the contribution to the HVC population from cooling-formation HVCs if tiny HVCs with  $V_{GSR} > 200$  km s $^{-1}$  can be shown to be distant ( $R > 50$  kpc).

## 6. CONCLUSION

The distributions of complexes in terms of their velocity and flux in the S-L06 simulations are consistent with HVC observations of the Milky Way and Andromeda, and point to neutral fractions above  $\sim 30\%$ . The neutral fraction implied by the Andromeda comparison is consistent with the neutral fraction implied by the Milky Way HVC comparison. This lower limit discredits a “tip-of-the-iceberg” picture of HVCs, wherein HVCs are dominantly an ionized phenomenon and the observed HI is just a small fraction of the baryonic mass of the clouds. The number of simulated complexes and their angular distribution on the sky is also consistent with the Milky Way HVCs, when the velocity selection effects and clustering effects are taken into account. The radial distribution of clouds is consistent with the Andromeda sample and, in particular, the lack of massive ( $\sim 10^6 M_\odot$ ) clouds at large radii ( $> 40$  kpc) in the simulation is consistent with observations of Andromeda which show a dearth of such clouds far from the disk. The physical and observational population characteristics of the simulated HVCs are consistent over 300 Myrs (excepting the nearest, most massive HVCs in the first snapshot) and are broadly independent of the point of observation chosen on the solar circle. We have shown that material condenses into HVCs from  $R = 10$  kpc to  $R = 100$  kpc in the halo, and that the HVCs have an overall accretion rate of  $\sim 0.2 M_\odot$ /year.

We have also shown that the velocity-distance domain is populated by simulated HVCs only in a specific region, and that all HVCs with known distances and unknown origins reside in this region. This points to a possible method for discriminating HVC origin given true space velocities. The simulated clouds would not always be identifiable as HVCs, as they may have low projected velocity. We find  $\sim 50\%$  of these halo clouds do not show high enough projected velocities to be considered HVCs. Distant simulated HVCs are typically less massive and slower moving than nearby simulated HVCs, implying a different distribution of physical parameters for distant CHVCs than for the nearby HVC population.

Observations using the Arecibo L-Band Feed Array will refine our understanding of both the Galactic HVC population with the GALFA-HI observing program (e.g. Peek et al. 2007 and Stanimirović et al. 2006) and the distribution of HVCs around other galaxies with the AGES observing program (e.g. Auld et al. 2006). Instruments coming online now, such as the Allen Telescope Array, will allow us to map the HI HVCs in the vicinity of other nearby galaxies with unprecedented efficiency and further compare these cooling-formation simulations to observed systems. In this way we may be able to determine whether there are characteristics of extra-galactic HVC systems that can inform our understanding of the formation of these galaxies and the variation in the character of their baryonic halos. In the more distant future, the Square Kilometer Array will allow us to extend this analysis to non-zero redshift, probing the cooling history of galaxies into the age of mergers.

The authors would like to thank Carl Heiles, Kathryn Peek, Evan Levine and Andrey Kravtsov for many helpful conversations. The TreeSPH simulations were performed on the SGI Itanium II facility provided by DCSC. The Dark Cosmology Centre is funded by the DNRFC. The research of JEGP was supported in part by NSF

grant AST04-06987.

## REFERENCES

- Auld, R., Minchin, R. F., Davies, J. I., Catinella, B., van Driel, W., Henning, P. A., Linder, S., Momjian, E., Muller, E., O'Neil, K., Sabatini, S., Schneider, S., Bothun, G., Cortese, L., Disney, M., Hoffman, G. L., Putman, M., Rosenberg, J. L., Baes, M., de Blok, W. J. G., Boselli, A., Brinks, E., Brosch, N., Irwin, J., Karachentsev, I. D., Kilborn, V. A., Koribalski, B., & Spekkens, K. 2006, *MNRAS*, 371, 1617
- Blitz, L., Spergel, D. N., Teuben, P. J., Hartmann, D., & Burton, W. B. 1999, *ApJ*, 514, 818
- Braun, R., & Burton, W. B. 1999, *A&A*, 341, 437
- de Avillez, M. A. 2000, *Ap&SS*, 272, 23
- Haardt, F., & Madau, P. 1996, *ApJ*, 461, 20
- Kalberla, P. M. W., Burton, W. B., Hartmann, D., Arnal, E. M., Bajaja, E., Morras, R., & Pöppel, W. G. L. 2005, *A&A*, 440, 775
- Kaufmann, T., Mayer, L., Wadsley, J., Stadel, J., & Moore, B. 2005, *ArXiv Astrophysics e-prints*
- Kulkarni, S. R., & Heiles, C. 1988, Neutral hydrogen and the diffuse interstellar medium (Galactic and Extragalactic Radio Astronomy), 95–153
- Lia, C., Portinari, L., & Carraro, G. 2002a, *MNRAS*, 335, 864
- . 2002b, *MNRAS*, 330, 821
- Maller, A. H., & Bullock, J. S. 2004, *MNRAS*, 355, 694
- Miville-Deschênes, M.-A., Boulanger, F., Reach, W. T., & Noriega-Crespo, A. 2005, *ApJ*, 631, L57
- Muller, C. A., Oort, J. H., & Raimond, E. 1963, *C. R. Acad. Sci. Paris*, 257, 1661
- Peek, J. E. G., Putman, M. E., McKee, C. F., Heiles, C., & Stanimirović, S. 2007, *ApJ*, 656, 907
- Putman, M. E. 2006, *ApJ*, 645, 1164
- Putman, M. E., Bland-Hawthorn, J., Veilleux, S., Gibson, B. K., Freeman, K. C., & Maloney, P. R. 2003, *ApJ*, 597, 948
- Putman, M. E., de Heij, V., Staveley-Smith, L., Braun, R., Freeman, K. C., Gibson, B. K., Burton, W. B., Barnes, D. G., Banks, G. D., Bhathal, R., de Blok, W. J. G., Boyce, P. J., Disney, M. J., Drinkwater, M. J., Ekers, R. D., Henning, P. A., Jerjen, H., Kilborn, V. A., Knezek, P. M., Koribalski, B., Malin, D. F., Marquarding, M., Minchin, R. F., Mould, J. R., Oosterloo, T., Price, R. M., Ryder, S. D., Sadler, E. M., Stewart, I., Stootman, F., Webster, R. L., & Wright, A. E. 2002, *AJ*, 123, 873
- Rocha-Pinto, H. J., Maciel, W. J., Scalo, J., & Flynn, C. 2000, *A&A*, 358, 850
- Seigar, M. S., Barth, A. J., & Bullock, J. S. 2006, *ArXiv Astrophysics e-prints*
- Sembach, K. R., Wakker, B. P., Savage, B. D., Richter, P., Meade, M., Shull, J. M., Jenkins, E. B., Sonneborn, G., & Moos, H. W. 2003, *ApJS*, 146, 165
- Sommer-Larsen, J. 2006, *ApJ*, 644, L1
- Sommer-Larsen, J., Götz, M., & Portinari, L. 2003, *ApJ*, 596, 47
- Springel, V., & Hernquist, L. 2002, *MNRAS*, 333, 649
- Stanimirović, S., Putman, M. E., Heiles, C., Peek, J. E. G., Goldsmith, P. F., Koo, B.-C., Krčo, M., Lazarian, A., Lee, J.-J., Mock, J. Muller, E., Pandian, J. D., Parsons, A., Tang, Y., & Werthimer, D. 2006, in press
- Thilker, D. A., Braun, R., Walterbos, R. A. M., Corbelli, E., Lockman, F. J., Murphy, E., & Maddalena, R. 2004, *ApJ*, 601, L39
- Thom, C., Putman, M. E., Gibson, B. K., Christlieb, N., Flynn, C., Beers, T. C., Wilhelm, R., & Lee, Y. S. 2006, *ApJ*, 638, L97
- Tripp, T. M., Wakker, B. P., Jenkins, E. B., Bowers, C. W., Danks, A. C., Green, R. F., Heap, S. R., Joseph, C. L., Kaiser, M. E., Linsky, J. L., & Woodgate, B. E. 2003, *AJ*, 125, 3122
- Tufte, S. L. 2004, in *ASSL Vol. 312: High Velocity Clouds*, ed. H. van Woerden, B. P. Wakker, U. J. Schwarz, & K. S. de Boer, 167
- Tufte, S. L., Wilson, J. D., Madsen, G. J., Haffner, L. M., & Reynolds, R. J. 2002, *ApJ*, 572, L153
- van Woerden, H., & Wakker, B. P. 2004, in *ASSL Vol. 312: High Velocity Clouds*, ed. H. van Woerden, B. P. Wakker, U. J. Schwarz, & K. S. de Boer, 195
- Wakker, B. P. 2001, *ApJS*, 136, 463
- Wakker, B. P. 2004, in *ASSL Vol. 312: High Velocity Clouds*, ed. H. van Woerden, B. P. Wakker, U. J. Schwarz, & K. S. de Boer, 25
- Wakker, B. P., & van Woerden, H. 1991, *A&A*, 250, 509
- Weiner, B. J., Vogel, S. N., & Williams, T. B. 2001, in *ASP Conf. Ser. 240: Gas and Galaxy Evolution*, 515
- Westmeier, T., Braun, R., & Thilker, D. 2005, *A&A*, 436, 101
- White, S. D. M., & Frenk, C. S. 1991, *ApJ*, 379, 52
- White, S. D. M., & Rees, M. J. 1978, *MNRAS*, 183, 341